Coalescence in Polymer Blends during Shearing

Su-Ping Lyu, Frank S. Bates, and Christopher W. Macosko
Dept. of Chemical Engineering and Materials Science, University of Minnesota, Minneapolis, MN 55455

Control of coalescence is a critical factor in preparing polymer blends with specific morphologies. Coalescence was studied as a function of shear rate, volume fraction, viscosity ratio, and amount of block copolymer in a model system comprising polystyrene (PS) and high density polyethylene (HDPE). Small drops of HDPE ($\sim 2\ \mu m$) were initially developed by shearing at 10 s^{-1} in a cup-cone shear cell for 20 min. The shear rate $\dot{\gamma}$ was then decreased to between 0.1 and 2.5 s^{-1}, and the state of coalescence was determined after quenching samples following specified periods of steady shearing. The PS portions of quenched samples were dissolved in chloroform, and the HDPE particles filtered from the suspension. These particles were imaged by scanning electron microscopy, which showed a sharp increase in the volume-average particle diameter at specific times that depend on shear rate volume fraction, and viscosity ratio. Little change was observed in the number average diameter (D_n) at low shear rates up to a total strain of 360. At higher shear rates, however, D_n significantly increased. Interestingly, adding small amounts of block copolymer to the blends significantly suppressed coalescence. These results are discussed in terms of particle trajectory and deformation during flow.

Introduction

Coalescence is a process in which two or more particles collide and physically merge into one particle. Two classes of coalescence play critical roles in the development of morphology during the processing of immiscible polymer blends. During flow, a steady-state balance between *flow driven coalescence* (Figure 1) and breakup produces a population of particles with a specific size distribution. Annealing leads to *static coalescence*, a mechanism that reduces interfacial area through particle-particle fusion. The relative importance of these two types of coalescence can be estimated based on the Peclet number $Pe = D^2\dot{\gamma}/\mathfrak{D}$ a ratio of the external flow to the movement due to Brownian motion, where D and $\mathfrak{D}$ are the particle diameter and diffusion coefficient, respectively. Flow-driven coalescence dominates when $Pe \gg 1$ (Wang, Zinchenko, and Davis, 1994).

Flow-driven coalescence actually is simpler to model than static coalescence; the driving forces for the latter are complicated by such factors as Brownian motion, van der Waals interactions, particle reshaping, and sedimentation. Thus, in some respects flow-driven coalescence is more suitable for studying the general mechanism of coalescence than the conventional static annealing. However, there are only a few reports of experimental studies that deal with flow-driven coalescence in polymer melts (Vinckier et al., 1998; Kim et al., 1998) relative to the extensive experimental efforts that have focused on static, or mixed static and flow-driven, coalescence in polymer and nonpolymer systems (Gillespie and Rideal, 1956; Charles and Mason, 1960a,b; MacKay and Mason, 1963; Jang et al., 1983; Elmendorp and van der Vegt, 1986; Crist and Nesarikar, 1995; Sundararaj and Macosko, 1995; Macosko et al., 1996; Søndergaard and Lyngaae-Jørgensen, 1996; Schoolenberg et al., 1996, 1998; Grizzuti and Bifulco, 1997; Minale et al., 1997; Tandon and Diamond, 1997). There are two principal reasons for this shortcoming. First, uniform high steady shear rates are difficult to maintain in polymer melts. Secondly, measuring particle size and distribution under flow is technically challenging.

This article describes an experimental study of flow-driven coalescence. Initially, a fine dispersion of molten high density polyethylene (HDPE) particles was created in a polystyrene (PS) melt by shearing blends at a high steady shear rate. Subsequently, coalescence was initiated by decreasing the shear rate to a lower value and shearing the blend for various times. At the initial higher shear rate, coalescence and breakup are dynamically balanced. Upon decreasing the shear rate, coalescence becomes the dominant process. In our study $Pe >$

Correspondence concerning this article should be addressed to F. S. Bates or C. W. Macosko.

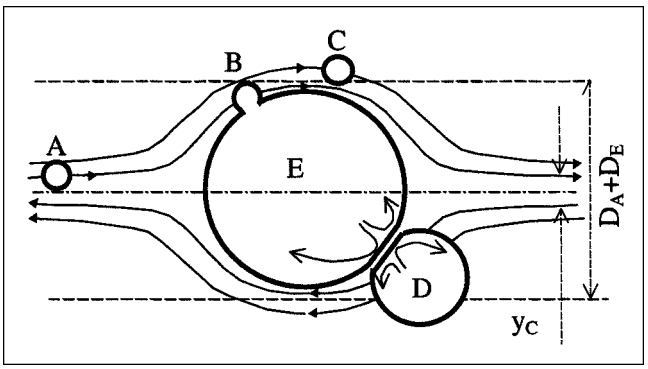

Figure 1. Particle-particle coalescence.

A small particle (A) moves towards a large particle (E) following a streamline and coalesces with it (B) or passes by, but does not coalescence (C). Particles deform when they approach to each other (D). Due to their motion along streamlines, only those particles within the region of y_c coalesce with the large one. Otherwise, all the particles in the region of $D_A + D_E$ would coalesce (where D_A and D_E are the particle diameters). The arrows inside the drops show the fountain flow.

1,000, coalescence is thus expected to be driven by flow. We used a cup-cone shear cell to achieve a relatively high initial shear rate $10s^{-1}$ that led to a fine particle morphology. Filtration and scanning electron microscopy (SEM) techniques were employed to measure particle size over a broad range (0.2–50 μm). Coalesence was studied as a function of shear rate, volume fraction of the dispersed phase, viscosity ratio, and the amount of added polystyrene-polyethylene (PS-PE) block copolymer. The block copolymer localized at the PS/HDPE interface thereby stabilized the morphology.

Experimental Studies

Materials and sample preparation

PS and HDPE used in this study were obtained from the Dow Chemical and Aldrich Chemical Companies. The PS-PE symmetric (50/50 vol) di-block copolymer was synthesized by Todd Jones using anionic polymerization and catalytic hydrogenation methods described elsewhere (Bates et al., 1989; Gehlsen, 1993). The number average molecular weights and polydispersity indices of these polymers were measured by gel permeation chromatography (GPC) and are listed in Table 1. Melt indices of PS and HDPE were provided by the manufacturers. The densities of PS and HDPE at 220°C, the temperature employed in the present study, were estimated to be 0.964 and 0.738 g/cm^3, respectively, based on values at 140°C reported by Fetters et al. (1994) and published thermal expansion coefficients by Brandrup and Immergut (1975) and Osswald (1998). The rheological properties of these materials were measured at 220°C with a dynamic stress rheometer (DSR, Rheometric Scientific) and are plotted in Figure 2. Note that the viscosity of HDEP2 nearly matches that of PS over the entire frequency range. Blends were prepared by dry-mixing PS and HDPE pellets (and PS-PE powder when appropriate) followed by mixing in a batch mixer (Haake) equipped with roller blades at 180°C and 50 rpm for 10 min followed by 10 rpm for 5 min. A 10 rpm setting corresponds to an average shear rate close to 10 s^{-1}. In order to prevent

Table 1. Polymer Blend Components

	M_n (kg/mol)*	M_w/M_n*	$\eta_{PE/PS}$ (0.1 s^{-1})†	Melt Index‡
PS	142	2.2	1.00	
HDPE1	18	4.8	2.60	4
HDPE2	11	7	1.05	12
HDPE3	11	3.7	0.53	25
HDPE4‖			0.26	42
PS-PE§	40	< 1.1		

*Measured with gel permeation chromatography based on polystyrene standard calibration.
†Ratio of complex viscosities at 220°C.
‡Measured by manufacturers at conditions of 190°C and 2.16 kg according to ASTM D1238, in g/10 min.
§50 vol. % of PS.
‖From Aldrich Chemical Co.

oxidation during processing, an anti-oxidation agent (Irganox 1010, Ciba-Geigy) was added to the mixture at a concentration of 0.05–0.1 wt. %.

Dynamic coalescence

A challenging aspect of this experimental program was sustaining high steady shear rates without material failure. Kim et al. (1998) reported shear rates as high as 50 s^{-1} with blends of poly(styrene-acrylonitrile)/poly(cyclohexyl methacrylate) using a conventional cone-plate device without inducing edge failure (fracture of the melt at the edge of the shear cell; see Macosko (1994) for details). We were not able to duplicate this result, and encountered edge failure when $\dot{\gamma} > 3$ s^{-1}. However, a modified design, illustrated in Figure 3, extended the attainable steady high shear rate. The bottom plate with a diameter of 25.00 mm was redesigned into a stainless steel cup with a diameter of 36 mm. This created a 4 mm gap between the cup and cone that was filled with polymer, thereby delaying edge failure until the shear rate reached 20 s^{-1}. This cup-cone shear cell was mounted in a Rheometrics RMS800 rheometer. All coalescence experiments were conducted at 220°C under N_2. PS/HDPE blends were initially

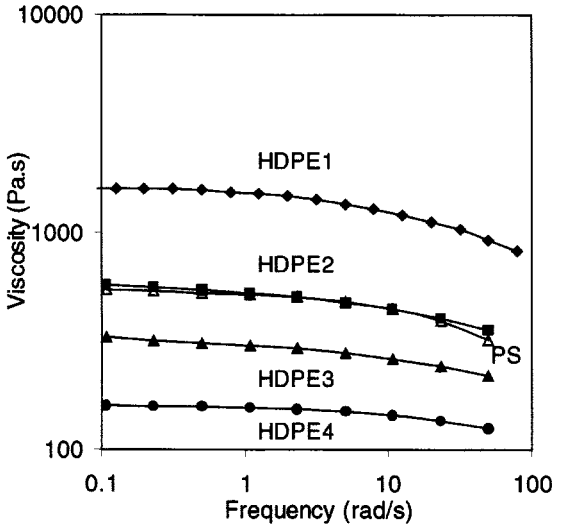

Figure 2. Complex viscosity of PS and HDPE vs. oscillation frequency at 220°C.

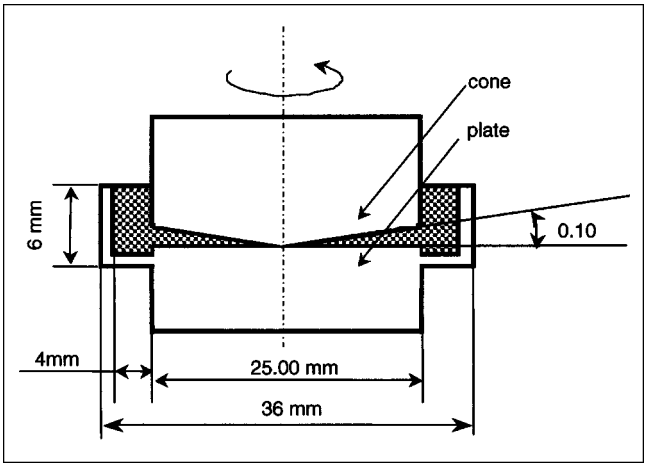

Figure 3. Cup-cone geometry for shearing polymer blends.

sheared at 10 s^{-1} for 20 min, followed by a reduction of the shear rate to a lower value for a predetermined time. Immediately after cessation of shearing, the sample was quenched by blowing cold N_2 gas on the fixture. Typically, 30 s was enough time to lower the temperature below 100°C, the T_g of the PS matrix, thereby fixing the morphology. The vitrified PS did not adhere to the stainless steel cup and cone, so the sheared polymer disk in the cup could be readily removed. Samples were cut out from the half radius position of the disk for subsequent particle-size measurements. Each coalescence time step requires a new loading.

There are two primary sources of experimental error in this coalescence procedure: (i) insufficient time to reach a steady-state initial morphology, and (ii) spurious coalescence during the quench. We have sheared blends at 10 s^{-1} for 10, 20, and 30 min in order to evaluate point (i) and found that the difference in particle size among these three times is less than 10%. Therefore, we assume that 20 min is sufficient time for blends to reach steady state at a shear rate of 10 s^{-1} or higher. We annealed a blend with 12.7 vol. % HDPE for 5 min prior to quenching with N_2 and found that the particle size changed less than 5% relative to the one cooled immediately after shear. Therefore, the 30 s quench time is assumed to be insignificant in our measurements.

We measured particle size by dissolving the PS matrix in chloroform at room temperature, and filtering the solution with a mixed cellulose acetate and nitrate filter with cut-off filtration size of 0.025 μm (Millipore, Inc.). The fact that chloroform dissolves PS, but does not affect the semicrystalline HDPE, was confirmed by measuring the particle sizes after 1 and 2 h of soaking in the solvent. The difference between particle sizes of these two extraction times was less than 5%. The typical time for HDPE in solvent was 1 h. The HDPE particles were collected on the filter, coated with 50 Å of platinum, and observed with a JEOL840 scanning electron microscope operated at 20 kV. The SEM was calibrated using a grating replica with 2,160 lines per millimeter (Ted Pella). Typically, 400 particles for each sample were imaged and analyzed using the NIH Image, version 1.61/ppc available on the WWW at (http://rbs.info.nih.gov/nih-image/about.html). We calculated both the volume and number average particle sizes using the equations

$$D_V = \Sigma\left(n_i D_i^4\right)/\Sigma\left(n_i D_i^3\right) \quad \text{and} \quad D_n = \Sigma\left(n_i D_i\right)/\Sigma n_i$$

where n_i is the number of particles with diameter of D_i. D_V mainly reflects the behavior of larger particles, while D_n reflects the behavior of smaller ones. We repeated several experiments three times and found D_V and D_n reproducible to $\pm 13\%$. The advantage of the filtration method is that it allows us to measure particles of a very broad size range (0.2–50 μm) for either dilute or concentrated polymer bends (Figure 4).

Results

Shear rates

Coalescence was carried out with a PS/HDPE2 (87.3/12.7 vol.) blend at 220°C at 3 different reduced shear rates: 0.1,

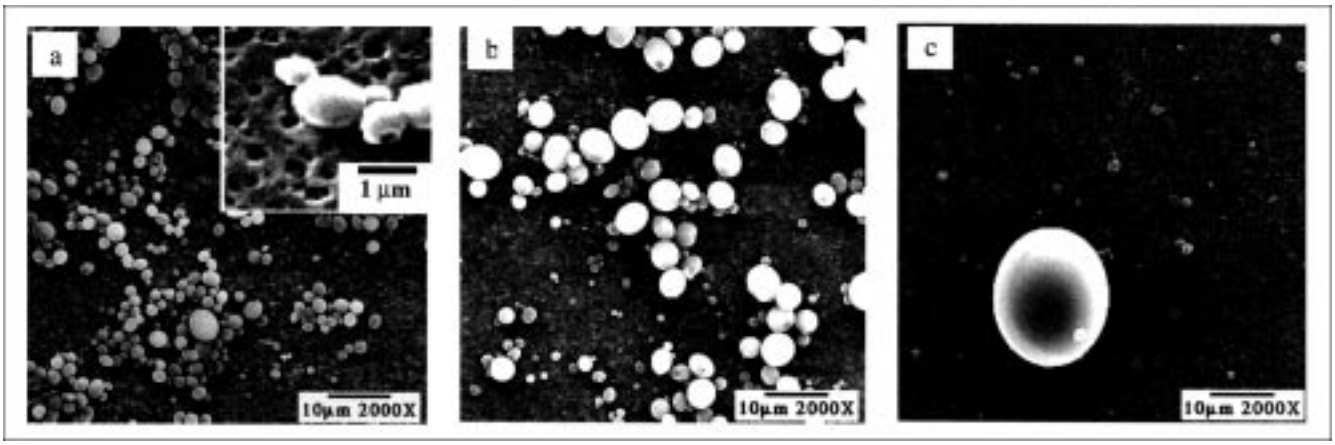

Figure 4. SEM images of particles in PS/HDPE (87.3/12.7) blend after coalescence at 0.1 s^{-1} for (a) 0, (b) 2, and (c) 60 min.

The inset picture in (a) indicates that the smallest particle that can be measured accurately is around 0.2 μm. It is possible for particles smaller than 0.2 μm to be trapped inside the holes of the filter.

1.0 and 2.5 s^{-1}. The viscosity ratio of HDPE2 to PS $\eta_{PE/PS}$ = 1.05 in this shear rate regime (Figure 2). Figure 4 shows the particles imaged at various stages of coalescence for the experiment at 0.1 s^{-1}. Most particles have a spherical shape. The first image shows that the initial morphology consists of relatively small particles with a rather narrow size distribution. After 2 min (12 units of strain) at the reduced shear rate of 0.1 s^{-1}, the particles are larger and the distribution broader (Figure 4b). After 60 min (360 units of strain) at 0.1 s^{-1}, a few large particles, and a greater number of small ones are evident, implying a very broad particle-size distribution (Figure 4c). However, the total volume of the larger particles is still much greater than that of the smaller ones. From images like these, D_V and D_n were calculated and these are plotted vs. total shear strain ($\dot{\gamma} \times time$) in Figure 5. For coalescence at 0.1 s^{-1}, D_V follows an "S shaped curve" behavior; at early stages, it increases with a coalescence strain slowly, then shows a sharp increase followed by a leveling off. Simultaneously, D_n shows little change.

For coalescence at shear rates of 1.0 and 2.5 (Figure 5), the changes in D_V with strain also display "S curves." However, coalescence at higher shear rates is slower, which is seen from the later onset of the rapid increase (larger onset strain γ_s) and smaller increase rate $dD_V/d\log(\gamma)$ (Table 2). Also, the equilibrium value of the volume average size decreases with shear rate. D_n for coalescence at 1.0 and 2.5 s^{-1} appear to increase with strain, although no clear trends can be deduced from these data.

Figure 6 shows some particle-size distributions. For clarity, we did not present all the data; instead, we selectively plot some typical distribution curves to show the main trends. At 0.1 s^{-1}, volume distribution curves shift towards large particles with coalescence, while number distribution shifts towards smaller particles up to a coalescence strain of 360. This indicates that the total number of particles is dominated by the smaller ones, while the total volume is controlled by the larger ones. For coalescence at 2.5 s^{-1}, the volume distribution shifts towards larger particles, which is similar to the $\dot{\gamma} = 0.1$ s^{-1} result. However, the number distribution changes little at first, then shifts towards the large particles at a strain of order 100. At 1.0 s^{-1}, the shift of volume distribution is similar to that at 0.1 and 2.5 s^{-1}. However, the number distribution is complicated: it first broadens, then shifts towards large particles at a large coalescence strain. Interestingly, a bimodal distribution appears in the intermediate stage. Also, at this shear rate, the largest increase in D_n was observed.

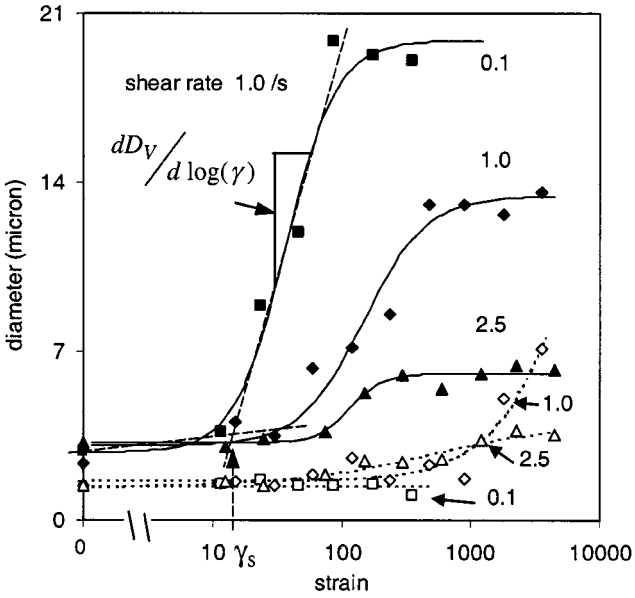

Figure 5. Volume (solid) and number (open) average diameters vs. total strain for coalescence at 0.1, 1.0, and 2.5 s^{-1}, respectively, in PS/HDPE2 (87.3/12.7) blends.

The lines are guides to the eye here and in subsequent figures. The onset strain γ_s and the rate of coalescence $dD_V/d\log(\gamma)$ at the onset of sharp increase in D_V are indicated by the long dashed lines.

Volume fraction

Coalescence was carried out at 0.1 s^{-1} in PS/HDPE2 blends that contained 6.4, 12.7 and 24.6 vol. % of HDPE2.

Table 2. Coalescence Results

Volume Fraction: PS/HDPE/PS-PE	η_{HDPE}/η_{PS} (0.1 s^{-1})*	Shear Rate (s^{-1})	D_{V0} (μm)†	$D_{V\max}$ (μm)‡	$\frac{D_{V0}}{D_n}$§	$\frac{D_{V\max}}{D_n}$§	γ_s‖	$\frac{dD_V}{d\log(\gamma)}$ (μm)#
87.3/12.7/0##	1.05	0.10	2.8	20	2.2	20	13	19
87.3/12.7/0	1.05	1.0	2.6	14	1.7	1.9	39	10
87.3/12.7/0	1.05	2.5	2.9	6.3	2.2	1.8	79	4.5
75.4/24.6/0	1.05	0.10	5.4	26	2.9	36	5.7	19
93.6/6.40/0	1.05	0.10	2.9	19	2.2	15	24	17
87.3/12.7/0	0.26	0.10	2.9	44	2.1	71	13	19
87.3/12.7/0	0.53	0.10	2.9	35	1.9	32	13	19
87.3/12.7/0	2.6	0.10	3.1	13	2.5	13	23	10
86.9/12.6/0.54	1.05	0.10	1.6	3.2	1.6	1.6		
86.3/12.6/1.1	1.05	0.10	1.6	1.8	1.6	1.7		

*Ratio of complex viscosities at 220°C.
†Initial volume average diameter.
‡Maximum volume average diameter.
§D_n is chosen at the same strain as D_{V0} or $D_{V\max}$.
‖Strain at the onset of sharp increase in D_V. See Figure 5 for definition.
#Rate of sharp increase in D_V. See Figure 5 for definition.
##Experiments were repeated three times with this blend. Deviation values in D_{V0}, $D_{V\max}$, and so on, are ±13%.

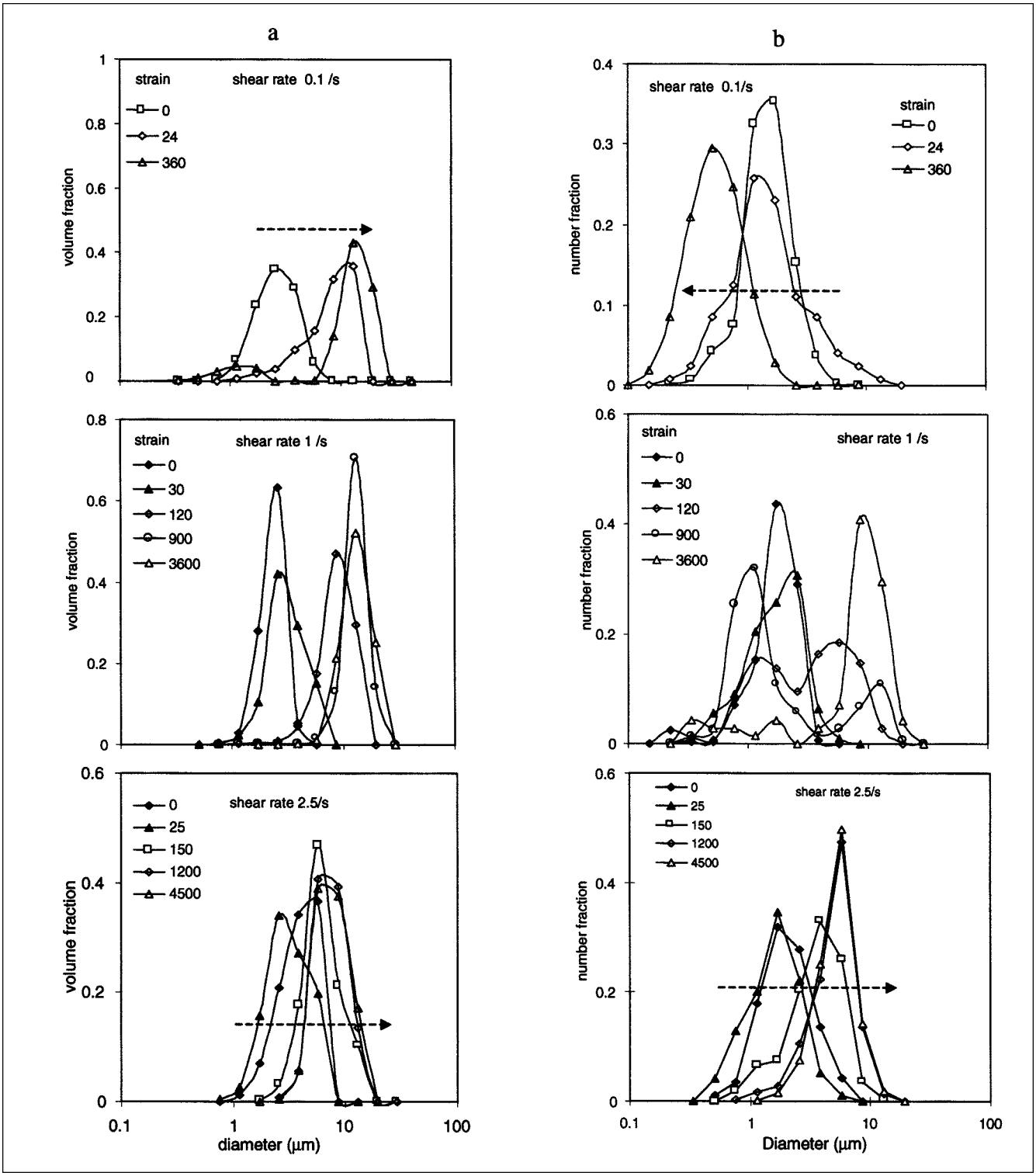

Figure 6. Evolution of volume (a) and number (b) particle-size distributions after coalescence at various shear rates in PS/HDPE2 (87.3/12.7) blends.

The arrows indicate the shift in the directions of the distribution.

Figure 7 shows the volume and number average particle diameters vs. coalescence strain. While the trends for D_V and D_n vs. strain are similar for all three volume fractions, the coalescence rate for higher volume fraction is faster, which is seen from the earlier onset, or smaller γ_s, of the rapid increase in D_V. This agrees with prior experiments indicating that higher volume fractions cause more coalescence (Sundararaj and Macosko, 1995). However, the values of

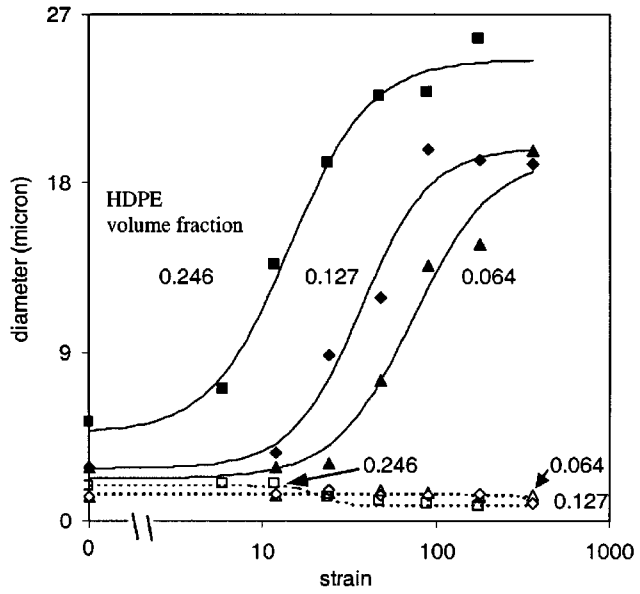

Figure 7. Effect of HDPE volume fraction.

Volume average (solid) and number (open) particle diameters vs. strain for coalescence at 0.1 s^{-1} in PS/HDPE2 blends with HDPE2 volume fraction of 6.4, 12.7, and 24.6%, respectively.

$dD_V/d\log(\gamma)$ are very close to each other (Table 2). Increasing the volume fraction mainly increases the collision frequency of particles. Thus, similar $dD_V/d\log(\gamma)$ means that the rate of increase in D_V is not sensitive to the collision frequency, although it depends on the shear rate as shown in the previous section. D_n changes very slowly for all these blends. Changes in particle-size distributions were similar to the results for the shear rate of 0.1 s^{-1}, shown in Figure 6. Specifically, the volume distribution curves shifted towards larger particles while the number distribution curves shifted towards smaller particles.

We plotted D_V vs. the product of strain and volume fraction ($\gamma \cdot \phi$), but the three curves of different volume fractions did not overlap very well. However, upon normalizing D_V by the initial values and plotting them again vs. $\gamma \cdot \phi$, a good superposition was observed (Figure 8).

Viscosity ratio

A third variable in our coalescence experiments is $\eta_{PE/PS}$, the ratio of the HDPE dispersed phase to the PS matrix viscosity. Figure 9 shows the evolution of particle diameters vs. coalescence strain for blends prepared with a single PS matrix (87.3%) and four different HDPEs yielding $\eta_{PE/PS}$ values of 0.26, 0.53, 1.05, and 2.6. Coalescence was carried out at 0.1 s^{-1}. The slowest increase in D_V with strain is obtained with the largest $\eta_{PE/PS}$ (2.6). Interestingly, the blends with $\eta_{PE/PS} = 0.26$, 0.53, and 1.05 exhibit a similar increase in D_V at the early stages, which is quantified by the values of γ_s and $dD_V/d\log(\gamma)$ (Table 2). This suggests that the dependence of D_V on $\eta_{PE/PS}$ is relatively weak in the regime $\eta_{PE/PS} \leq 1$. Once again, D_n changes only slightly with coalescence up to a strain of 360 for all values of $\eta_{PE/PS}$.

Block copolymer

The effects of added PS-PE di-block copolymer on coalescence in the PS/HDPE2 (87.3/12.7 vol.) blends at 0.1 s^{-1} are shown in Figure 10. In contrast to the sharp increase in D_V in the absence of PS-PE, the D_V in blends containing 1.1 vol. % PS-PE shows almost no change with strain. In blends containing 0.5 vol. % PS-PE, D_V increases from 1.6 to only 3.2

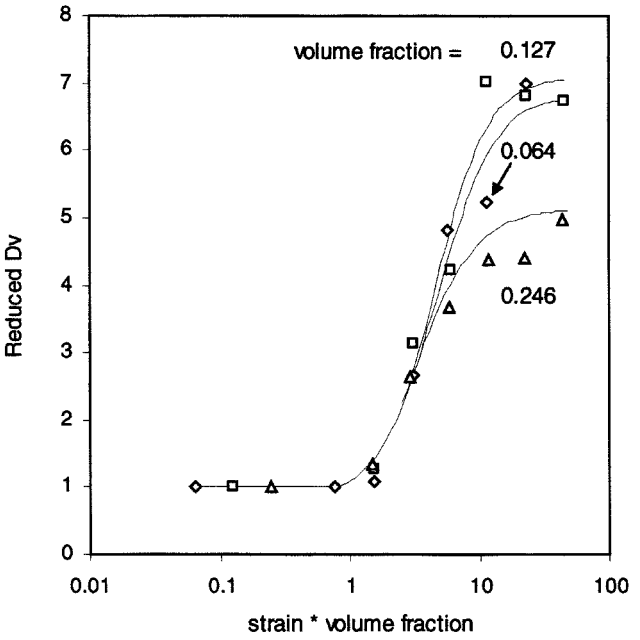

Figure 8. Normalized D_V by their initial values vs. the product of strain and volume fraction for the coalescence in PS/HDPE2 blend at 0.1 s^{-1}.

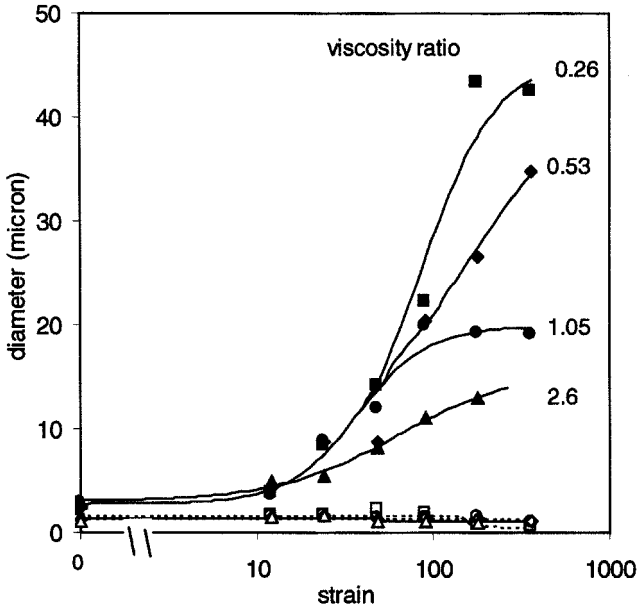

Figure 9. Effect of viscosity ratio.

Volume (solid) and number (open) average particle diameters vs. strain for coalescence at 0.1 s^{-1} in PS/HDPE (87.3/12.7) blends with viscosity ratios of 0.26, 0.53, 1.05, and 2.6.

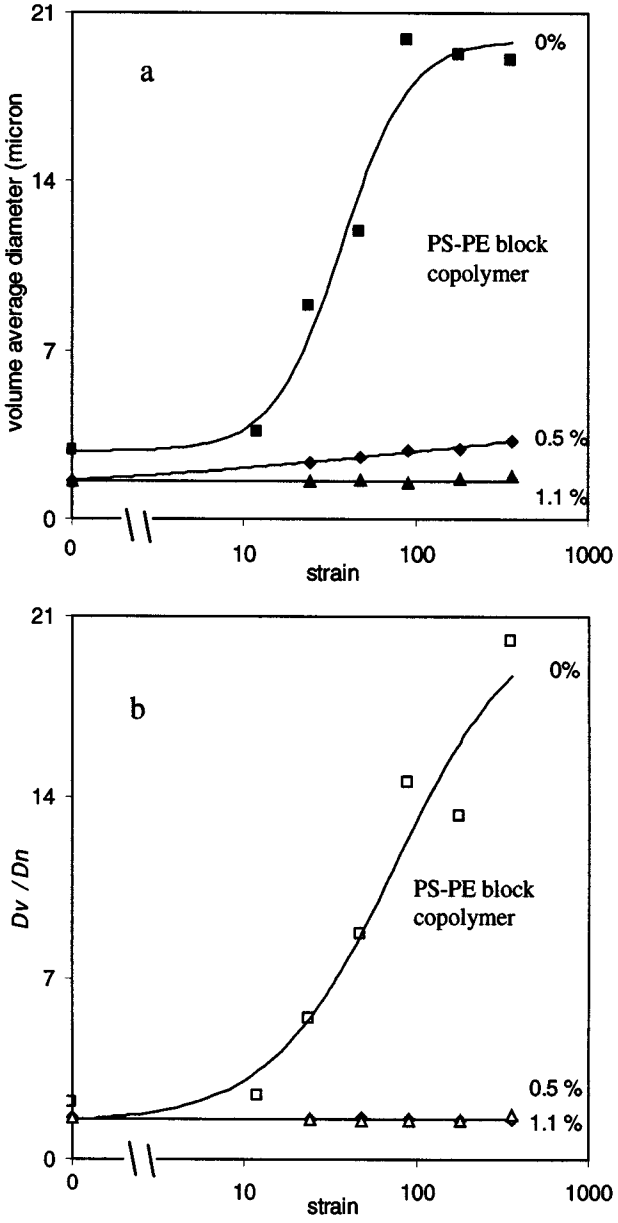

Figure 10. Effect of block copolymer.

Volume average particle diameter (a) and broadness of the particle distribution (D_V/D_n); (b) vs. strain in PS/HDPE2 (87.3/12.7) blends at 0.1 s^{-1} containing 0, 0.5, and 1.1 vol. % block copolymer.

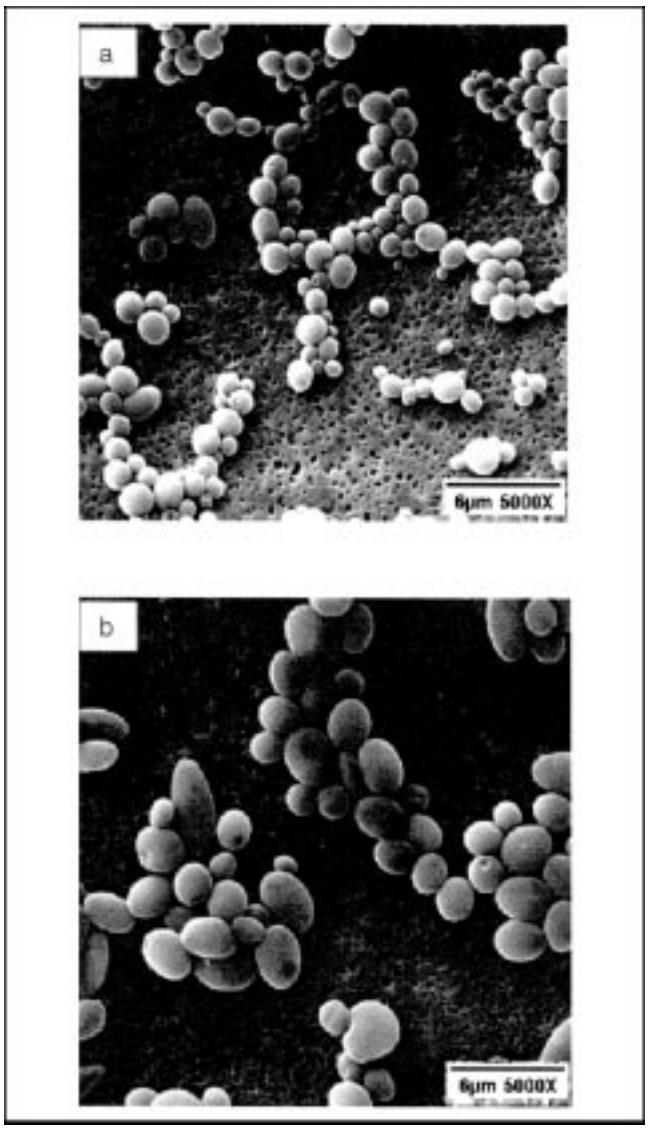

Figure 11. Particles from a blend containing 0.5 vol. % block copolymer (a) before coalescence; $D_{V0} = 1.6$ μm and (b) after coalescence at 0.1 s^{-1} for a strain of 360, $D_V = 3.2$ μm.

μm after coalescence for a strain of 360. These results unambiguously demonstrate that block copolymer significantly suppresses coalescence in PS/HDPE2 blends.

The presence of PS-PE also greatly reduces the breadth of the particle-size distribution during coalescence. We use the ratio of volume average particle size to number average (D_V/D_n) to represent the breadth of the particle-size distribution. Figure 10b shows that D_V/D_n for blends without PS-PE increases from 2 to almost 20, while D_V/D_n remains nearly constant at 1.6 for the blends containing 0.5 and 1.1% of PS-PE. This effect can be seen more by comparing the particle images of a blend containing 0.5% PS-PE (Figure 11) to that without PS-PE (Figure 4). Particles in the blend with PS-PE are smaller and narrowly distributed after coalescence for a strain of 360 in sharp contrast to that without PS-PE (Figure 4c).

Block copolymers also reduced initial particle sizes. The addition of 0.5 or 1.1% PS-PE reduced D_V by almost a factor of 2, from 2.9 to 1.6 μm (Table 2). However, the reduction of the particle size by the addition of a block copolymer is less significant than the nearly complete suppression of coalescence.

It is also worth pointing out that, in the blends without block copolymers, D_V is always larger than that predicted by Taylor (1932) theory $Ca = D\eta_m\dot{\gamma}/(2\Gamma)$, where Ca is the critical capillary number, reported to be about 0.2 for Newtonian fluids (Barthes-Biesel and Acrivos, 1973). η_m is the viscosity of the matrix (PS) and Γ is the interfacial tension. For example, D_V was measured to be 2.9 μm for a blend with 12.7 vol.

% HDPE at 10 s^{-1}. Using $\eta_m = 610$ Pa·s (Figure 2) and $\Gamma = 5$ mN/m (Elemans, Janssen, and Meijer, 1990), Taylor theory predicts $D \approx 0.3$ μm, about ten times smaller than measured. This large difference is due to particle coalescence (Sundararaj and Macosko, 1995).

Discussion

Vinckier et al. (1998) have published studies of flow-driven coalescence in PIB/PDMS blends as a function of shear rate and volume fraction of dispersed phase of the blend. They measured D_V by optical microscopy and rheological methods. They found that D_V vs. strain increases faster at a lower shear rate and with higher volume fractions of dispersed phase. These results qualitatively agree with ours. However, due to the resolution limit of optical microscopy, they could not obtain accurate measurements for small particles. They reported $D_V/D_n < 1.3$ after coalescence, considerably smaller than what we found in our experiments; $D_V/D_n \approx 20$ after 60 min of coalescence at 0.1 s^{-1}. Our filtration method is made possible by the solubility differences between PS and HDPE and the rigidity of HDPE at ambient temperature which allowed use of SEM. With the filtration method, we can accurately measure particle size down to 0.2 μm. Furthermore, in our experiments, we used a cup-cone shear cell, which permitted us to create fine particles at 10 s^{-1} and to carry out coalescence at shear rate reduction ratios up to 100 (10 down to 0.1 s^{-1}). Both of these parameters are higher than those used in the Vinckier et al. experiments where the highest shear rate and reduction ratio were 4.5 s^{-1} and 30, respectively. We have also studied the effects of viscosity ratio and block copolymers on coalescence.

It can be easily understood that coalescence becomes faster with increasing volume fraction of particle phase as a result of higher collision frequency induced by higher particle concentration. Good superposition among the curves of normalized D_V vs. $\gamma \cdot \phi$ (Figure 8) supports this result (Vinckier et al., 1998). The similar increase of D_V with strain (see the $dD_V/d\log(\gamma)$ in Table 2) for different volume fraction suggests that the coalescence efficiency does not change significantly with volume fraction.

The fact that higher shear rates cause a delay in the increase in D_V might be because higher shear rates reduce particle interaction time and also result in a stronger resistant interaction between coalescing particles. This resistance is illustrated in Figure 1D where the squeezing flow of the matrix between two coalescing particles causes them to flatten at the region of closest approach. This deformation, increasing with increasing shear rate, causes resistance to a closer approach. As a result, particle coalescence is delayed with increasing shear rate. It should be noted that this is a local deformation that increases as particles come closer. Particles can also deform as a whole due to the shear field around it. However, this usually is smaller than the local deformation (Wang et al., 1994).

Another interesting point is that, at low shear rates, D_V shows a sharp increase while D_n changes only slightly, regardless of volume fraction or viscosity ratio. As shown in the particle-size distribution plots (Figure 6), the total number of smaller particles is much greater than that of larger ones after coalescence at 0.1 s^{-1} for a strain of 360, although the total volume of the smaller ones is much less than that of the larger ones. This means that the smaller particles coalesce much slower with either themselves or the larger ones. Large particles have a big capture radius for collision; therefore, coalescence should be fast as long as large particles are involved. If so, the smaller particles should quickly coalesce with the larger ones. However, this disagrees with the slow increase in D_n and the relative increase in the number of small particles after coalescence at a lower shear rate. The discrepancy here suggests that the coalescence rate between large and small particles is reduced. Such reduction in coalescence rate between large and small particles results from the fact that the small particles tend to follow the streamlines around the large particles (droplet C in Figure 1). This causes the small particles to change their trajectories. Some of them just pass by the large particle rather than collide with it. As a result, the coalescence rate is decreased. This effect is not expected to be significant in coalescence, where the final particle size does not differ too much from the initial size or the shear rate reduction ratio is small. This might be one reason for the fairly fast increase of D_n in coalescence at 2.5 s^{-1}, where the number distribution shifts towards large particles. It should be pointed out that this discussion is limited to the early stage of the shear rate reduction process. The number distribution is expected to shift towards the large particles when the morphology approaches steady state after a long enough time of coalescence. This could be another reason for the number distribution shifting towards large particles in the late stage of coalescence at 2.5 s^{-1} where the morphology changes slowly, suggesting being close to a steady state.

Effects of viscosity ratio on coalescence are complicated. When the viscosity of particles is high, the fountain flow inside particles is reduced (droplet D in Figure 1). This increases the resistance for particles to approach each other and, thus, reduces the coalescence rate. This agrees with our experimental results at viscosity ratios of 1.05 and 2.6. However, our experiments show that coalescence rate is essentially unchanged for viscosity ratios less than 1. The reasons for this are not obvious, although it suggests that the effects of viscosity ratio on particle deformation, fountain flow, and trajectory might cancel each other. Modeling particle collision becomes complex when both trajectory and deformation are relevant (Manga and Stone, 1993, 1995; Zhang et al., 1993; Rother et al., 1997).

Addition of block copolymer significantly suppresses coalescence, a result easily rationalized based on the accepted surface activity in the limit of strong segregation (Paul and Newman, 1978; Leibler, 1998). In close analogy with oil, water, and surfactant mixtures, the block copolymer is perceived to reduce the interfacial tension between PS and HDPE, and also to provide a steric barrier to particle fusion. However, the PS-PE does not seem to reduce very much the steady-state particle sizes. This result supports the idea that addition of block copolymer reduces particle size by suppressing coalescence more than by decreasing interfacial tension (Sundararaj and Macosko, 1995; Macosko et al., 1996). Milner and Xi (1996) suggest that when two particles approach each other, the block copolymers at interfaces are swept out of the gap. This leads to a strong repulsive force. As a result, coalescence is significantly suppressed. Milner and Xi also argued

that reduction of interfacial tension due to presence of block copolymer was small.

It should be pointed out that Kim et al. (1998) also observed that flow-driven coalescence rates in poly(styrene-acrylonitrile)/poly(cyclohexyl methacrylate) blends were reduced by the addition of poly(styrene-b-methyl methacrylate) block copolymer. Interestingly, they observed that particle-size distributions became narrower with coalescence, even in blends without block copolymers. This does not agree with either our results or those of Vinckier et al. (1998).

The focus of this article is the experimental study of coalescence. A modeling study of coalescence based on the theories of Smoluchowski (1917), Chesters (1991), and Wang et al. (1994) will be presented in another article (Lyu et al., 2000).

Conclusion

Polystyrene/high density polyethylene (PS/HDPE) blends were sheared at 10 s^{-1} using a cone-cup shear cell until a steady-state dispersed morphology was achieved. Subsequent reductions to a lower steady shear rate resulted in flow-driven particle coalescence. HDPE particles were isolated by dissolution of the PS matrix followed by filtration and imaging by scanning electron microscopy. Particle size and size distributions were measured at various shear rates, viscosity ratios (particle vs. matrix), volume fractions, and amounts of added PS-PE block copolymer, each as a function of shear strain ranging from 360 to 4,500 units. We believe that this is the most extensive study of polymer coalescence to date.

Volume average particle sizes displayed sharp increases with coalescence at specific strains, indicating the onset of coalescence. Higher onset strain suggests slower coalescence. Experiments show that the coalescence vs. strain slows down with increasing shear rate, decreasing volume fraction, and increasing viscosity ratio. Little change was observed in the number average particle size at low shear rates up to a total strain of 360. However, at higher shear rates, it significantly increases with coalescence. When a small amount of PS-PE block copolymer was added to the blends, coalescence is nearly completely suppressed. These results were explained in terms of hydrodynamic interactions related to particle trajectory and deformation during flow.

Acknowledgment

This work was supported by NSF (CTS9527940). The authors thank Todd Jones for the synthesis of the PS-PE block copolymer, David Giles, Milan Maric, and Damon Wickum for technical help, Todd Jones, Russell Hooper, David Morse, and MooSong Lee for helpful discussions, and Steven Hahn, the Dow Chemical Company, for providing the HDPE and PS samples.

Literature Cited

Allan, R. S., and S. G. Mason, ''Effects of Electric Field on Coalescence in Liquid+Liquid Systems,'' *Trans. Faraday Soc.*, **57**, 2027 (1961).

Barthes-Biesel, D., and A. Acrivos, ''Deformation and Burst of a Liquid Droplet Freely Suspended in a Linear Shear Field,'' *J. Fluid Mech.*, **61**, 1 (1973).

Bates, F. S., J. H. Rosedale, H. E. Bair, and T. P. Russell, ''Synthesis and Characterization of a Model Saturated Hydrocarbon Diblock Copolymer,'' *Macromol.*, **22**, 2557 (1989).

Brandrup, J., and E. H. Immergut, eds., *Polymer Handbook*, Wiley, New York (1975).

Crist, B., and A. R. Nesarikar, ''Coarsening in Polyethylene-Copolymer Blends,'' *Macromol.*, **28**, 890 (1995).

Chesters, A. K., ''The Modeling of Coalescence Processes in Fluid-liquid Dispersions: a Review of Current Understanding,'' *Trans. IchemE.*, **69**, 259 (1991).

Charles, G. E., and S. G. Mason, ''The Mechanism of Partial Coalescence of Liquid Drops at Liquid/Liquid Interfaces,'' *J. Colloid Sci.*, **15**, 105 (1960).

Charles, G. E., and S. G. Mason, ''The Coalescence of Liquid Drops with Flat Liquid/Liquid Interfaces,'' *J. Colloid Sci.*, **15**, 236 (1960).

Elemans, P. H. M., J. M. H. Janssen, and H. E. H. Meijer, ''The Measurement of Interfacial Tension in Polymer/polymer Systems: the Breaking Thread Method,'' *J. Rheol.*, **34**, 1311 (1990).

Elmendorp, J. J., and A. K. van der Vegt, ''A Study on Polymer Blending Microrheology: IV. Influence of Coalescence on Blend Morphology Origination,'' *Poly. Eng. Sci.*, **26**, 1322 (1986).

Fetters, L. J., D. J. Lohse, D. Richter, T. A. Witten, and A. Zirkel, ''Connection Between Polymer Molecular Weight, Density, Chain Dimension, and Melt Viscoelastic Properties,'' *Macromol.*, **27**, 4639 (1994).

Gehlsen, M. D., ''Catalytic Hydrogenation of Polymers: Synthesis and Characterization of Model Polyolefins,'' PhD Thesis, Univ. of Minnesota, Minneapolis (1993).

Gillespie, T., and E. K. Rideal, ''The Coalescence of Drops at an Oil-water Interface,'' *Trans. Faraday Soc.*, **52**, 173 (1956).

Grizzuti, N., and O. Bifulco, ''Effects of Coalescence and Break-Up on the Steady-state Morphology of an Immiscible Polymer Blend in Shear Flow,'' *Rheol Acta*, **36**, 406 (1997).

Jang, B. Z., D. R. Uhlmann, and J. B. Vander Sande, ''The Postdispersion Coalescence Phenomenon in Polymer-polymer Blends,'' *Rubber Chem. Tech.*, **57**, 291 (1983).

Kim, J. R., A. M. Jamieson, S. D. Hudson, I. Manas-Zloczower, and H. Ishida, ''Influence of Exothermic Interaction on the Morphology and Droplet Coalescence of Melt-mixed Immiscible Polymer Blends Containing a Block Copolymer,'' *Macromol.*, **31**, 5383 (1998).

Leibler, L., ''Emulsifying Effects of Block Copolymers in Incompatible Polymer Blends,'' *Macromol. Chem. Macromol. Symp.*, **15**, 1 (1988).

Lyu, S.-P., C. W. Macosko, and F. S. Bates, ''Modeling Shear Induced Coalescence in Polymer Blends,'' in press (2000).

MacKay, G. D., and S. G. Mason, ''The Gravity Approach and Coalescence of Fluid Drops at Liquid Interfaces,'' *Can. J. Chem. Eng.*, 203 (Oct., 1963).

Macosko, C. W., *Rheology: Principles, Measurements and Applications*, Wiley/VCH Publishers, New York, p. 215 (1994).

Macosko, C. W., P. Guégan, A. K. Khandpur, A. Nakayama, P. Marechal, and T. Inoue, ''Compatibilizers for Melt Blending: Premade Block Copolymers,'' *Macromol.* **29**, 5590 (1996).

Manga, M., and H. A. Stone, ''Buoyancy-Driven Interactions between Two Deformable Viscous Drops,'' *J. Fluid Mech.*, **256**, 647 (1993).

Manga, M., and H. A. Stone, ''Collective Hydrodynamics of Deformable Drops and Bubbles in Dilute Low Reynolds Number Suspensions,'' *J. Fluid Mech.*, **300**, 231 (1995).

Milner, S. T., and H. W. Xi, ''How Copolymers Promote Mixing of Immiscible Homopolymers,'' *J. Rheol.*, **40**, 663 (1996).

Minale, M., P. Moldenaers, and J. Mewis, ''Effect of Shear History on the Morphology of Immiscible Polymer Blends,'' *Macromol.*, **30**, 5470 (1997).

Osswald, T. A., *Polymer Processing Fundamentals*, Hanser Publishers, Munich (1998).

Paul, D. R., and S. Newman, eds., *Polymer Blends*, Vol. 2, Academic Press, New York (1978).

Rother, M. A., A. Z. Zinchenko, and R. H. Davis, ''Buoyancy-Driven Coalescence of Slightly Deformable Drops,'' *J. Fluid Mech.*, **346**, 117 (1997).

Schoolenberg, G. E., F. During, and G. Ingenbleek, ''Coalescence Measurements for PS (polystyrene) Matrix Blends Using the Spinning Drop Apparatus,'' *Macromol. Symp.*, **112**, 107 (1996).

Schoolenberg, G. E., F. During, and G. Ingenbleek, ''Coalescence and Interfacial Tension Measurement for Polymer Melts: Experiments on a PS-PE Model System,'' *Polymer*, **39**, 765 (1998).

Smoluchowski, V., ''Versuch einer Mathematischen Theorie der Koagulationskinetik Kollider Losungen,'' *Z. Phys. Chem.*, **92**, 129 (1917).

Søndergaard, K., and J. Lyngaae-Jørgensen, ''Coalescence in an Interface-Modified Polymer Blend as Studied by Light Scattering Measurements,'' *Polymer*, **37**, 509 (1996).
Sundararaj, U., and C. W. Macosko, ''Drop Break-Up and Coalescence in Polymer Blends: the Effects of Concentration and Compatibilization,'' *Macromol.*, **28**, 2647 (1995).
Tandon, P., and S. L. Diamond, ''Hydrodynamic Effects and Receptor Interactions of Platelets and Their Aggregates in Linear Shear Flow,'' *Biophysical J.*, **73**, 2819 (1997).
Taylor, G. I., ''The Viscosity of a Fluid Containing Small Drops of Another Fluid,'' *Proc. R. Soc. London, Ser. A*, **138**, 41 (1932).
Vinckier, I., P. Moldenaers, A. M. Terracciano, and N. Grizzuti, ''Droplet Size Evolution during Coalescence in Semiconcentrated Model Blends,'' *AIChE J.*, **44**, 951 (1998).
Wang, H., A. Z. Zinchenko, and R. H. Davis, ''The Collision Rate of Small Drops in Linear Flow Fields,'' *J. Fluid Mech.*, **265**, 161 (1994).
Zhang, X. G., R. H. Davis, and M. F. Ruth, ''Experimental Study of Two Interacting Drops in an Immiscible Fluid,'' *J. Fluid Mech.*, **249**, 227 (1993).

Manuscript received Apr. 1, 1999, and revision received Sept. 29, 1999.